ACS OMEGA

http://pubs.acs.org/journal/acsodf

Article

Poly-L-lysine/Sodium Alginate Coating Loading Nanosilver for Improving the Antibacterial Effect and Inducing Mineralization of Dental Implants

Chuchu Guo,[†] Wendi Cui,[†] Xiaowei Wang,[†] Xiaoxuan Lu, Lulu Zhang, Xiangyang Li, Wei Li, Weibo Zhang, and Jialong Chen*

Cite This: *ACS Omega* 2020, 5, 10562−10571

Read Online

ACCESS | Metrics & More | Article Recommendations

ABSTRACT: In recent years, antibacterial surface modification of titanium (Ti) implants has been widely studied in preventing implant-associated infection for dental and orthopedic applications. The purpose of this study was to prepare a composite coating on a porous titanium surface for infection prevention and inducing mineralization, which was initialized by deposition of a poly-L-lysine (PLL)/sodium alginate(SA)/PLL self-assembled coating, followed by dopamine deposition, and finally in situ reduction of silver nanoparticles (AgNPs) by dopamine. The surface zeta potential, SEM, XPS, UV−vis, and water contact angle analyses demonstrate that each coating was successfully prepared after the respective steps and that the average sizes of AgNPs were 20−30 nm. The composite coating maintained Ag^+ release for more than 27 days in PBS and induced mineralization when incubated in SBF. The antibacterial results showed that the composite coating inhibited/killed bacteria on the material surface and killed bacteria around them. In addition, although this coating inhibited the initial adhesion of osteoblasts, the mineralized surface greatly enhanced the cytocompatibility. Thus, we concluded that the composite coating could prevent bacterial infections and facilitate mineralization *in vivo* in the early postoperative period, and then, the mineralized surface could enhance the cytocompatibility.

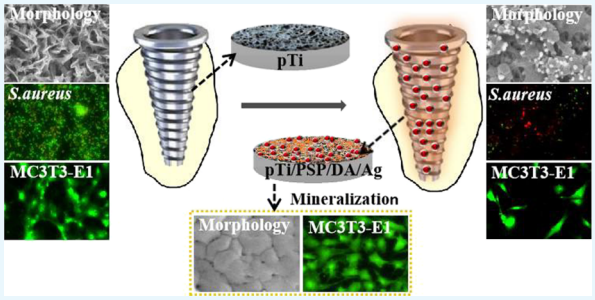

INTRODUCTION

In recent years, commercial Ti and its alloys have been applied in orthopedic fixation, prosthesis, oral implants, and other medical devices due to their excellent biocompatibility, low elastic modulus, and long-term stability.[1−3] However, insufficient osseointegration and the lack of antibacterial capabilities increase the chance of implant failure, which represents a major challenge for the application of titanium-based implant devices.[4] To improve the biological performance of Ti implants, different surface modification methods have been applied, including sandblasting processing, acid etching, alkaline treatment, plasma spraying, oxidization, and so on.[5,6] Among the above methods, the alkali-heated treatment is most commonly used for preparing micro/nanoporous microstructures with a high surface area to improve the cytocompatibility[7] and corrosion resistance[8] of titanium implants.

Electrostatic self-assembly is a technique based on the successive adsorption of polyanions and polycations on the surface of a material through electrostatic interactions. This technique is a flexible, simple method for a functionalizing surface[9−12] to combine two or more desirable properties of biomaterials. Our previous studies have indicated that heparin/collagen self-assembly coating could improve blood compatibility and cytocompatibility of titanium.[13,14] Moreover, the thickness and the degradation of this coating could influence these biological properties of a titanium surface.[15]

In addition to cytocompatibility, bacterial infection is another focus of implant construction, which can lead to implant failure and high costs. The method for endowing implants with antibacterial property involves combining implants with antibacterial substances containing antibiotics (e.g., gentamicin and vancomycin), antiseptics (e.g., chlorhexidine), and metals (e.g., gold and copper).[16−19] Silver and silver nanoparticles (AgNPs) have long been used as antibacterial agents in the application of dental/orthopedic materials,[20,21] wound dressings,[22] and food packaging[23] due to their antibacterial activity against a broad spectrum of bacteria and low bacterial resistance. There are many ways to incorporate silver nanoparticles onto a titanium surface to

Received: March 4, 2020
Accepted: April 23, 2020
Published: May 4, 2020

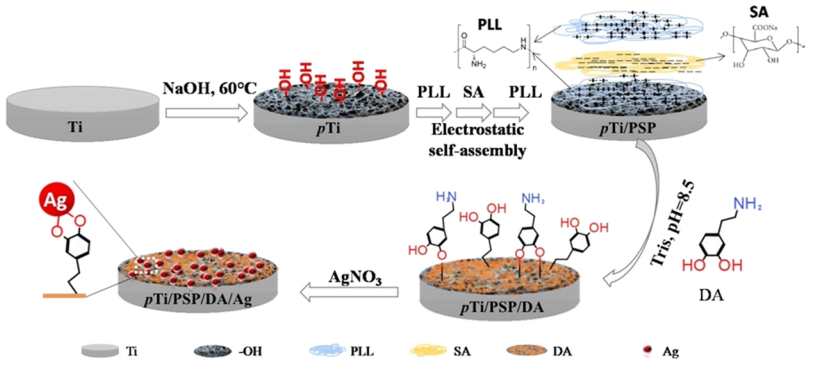

Figure 1. Schematic illustration for each step.

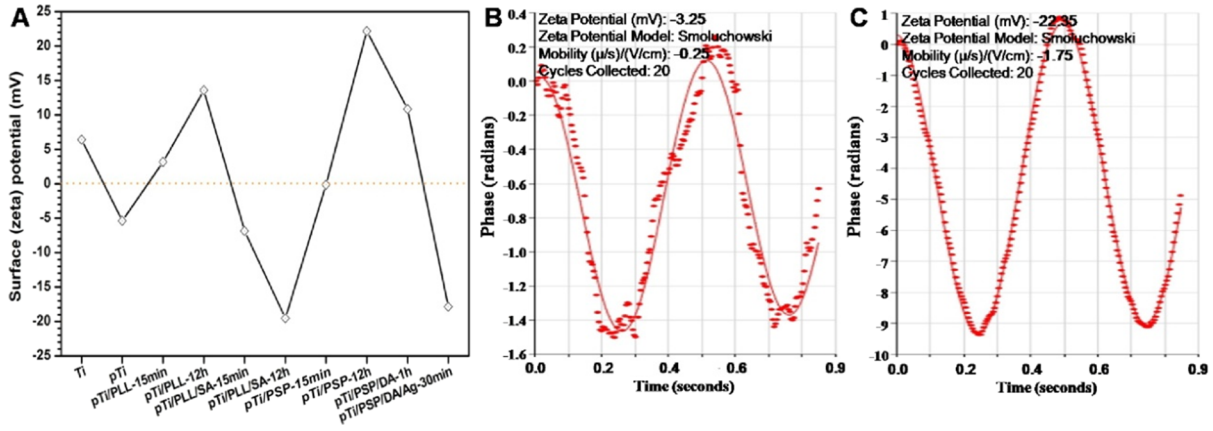

Figure 2. (A) Surface zeta potential (SZP) of different surfaces. (B) Zeta potential of dopamine particle. (C) Zeta potential of AgNPs.

obtain antibacterial properties, including sputtering deposition, coating carrier method, plasma immersion implantation, etc.[24−26]

Dopamine can form polydopamine coatings on various surfaces by oxidative self-polymerization,[27] while exposed functional groups (e.g., catechol and amine) could be used for secondary reactions with covalent graft biomolecules,[28] in situ reduction of metal ion,[21,29] and chelation of Ca^{2+} ions to form a mineralized layer.[21,30] Several studies have shown that the dopamine coatings could enable chelation of Ag^{+} and reduce them to form Ag^{0}, which is an effective way to obtain antibacterial ability, but the cytotoxicity of silver should be considered.[21,30] In addition, dopamine can induce mineralization to enhance the osteoblast compatibility.[21]

In this report, we synthesized a silver-loaded composite coating via polyelectrolyte electrostatic self-assembly as well as reduction of silver with dopamine. Poly-L-lysine (PLL) can enhance its interactions with cells through electrostatic interactions and promote cell adhesion.[31] Sodium alginate (SA) has been extensively applied in tissue engineering[32] and drug delivery systems[33] to improve antibacterial properties by incorporating antibacterial agents (e.g., quaternary ammonium). We prepared PLL/SA/PLL (PSP) polyelectrolyte coating on an alkali heat-treated titanium surface to improve cytocompatibility, then the coating was modified with a polydopamine in the dopamine solution, and finally in situ reduced Ag^{+} to form AgNPs on the surface by immersing samples in $AgNO_3$ solution (Figure 1). The results indicated that incorporating the PSP coating could improve cytocompatibility; the AgNP-modified surface possessed an excellent antibacterial effect and low cytotoxicity. However, this coating could promote mineralization and then improve cytocompatibility greatly. This design enabled the preparation of a silver-loaded composite coating by a simple method (dip coating) and provided the implant surface with antibacterial ability and induced mineralization, which could be potentially valuable for dental- and orthopedic-related applications.

RESULTS AND DISCUSSION

Surface Physicochemical Characterization. The main driving force for electrostatic assembly on the surface is the surface charge reversal that happens after each deposition procedure. Thus, the surface zeta potential (SZP) of the different surfaces was measured. As shown in Figure 2A, the SZP value of the pure titanium (Ti) was 6.43 mV and it was −5.4 mV after alkali-heat treated titanium (pTi) because the alkali-heat treatment produced a large number of hydroxyl groups on the surfaces.[15] The SZP value was changed with the charge of the polyelectrolyte layers deposited on the surface. Moreover, we investigated the effect of immersion time of different Ti plates in polyelectrolyte solutions on the SZP. The results indicated that the negative potential of pTi/PLL/SA or the positive potential of the pTi/PLL and pTi/PSP for immersion for 12 h was more than that of them for immersion for 15 min. Compared with the short immersion time, the surface may achieve steady-state conditions with a long immersion time, which indicated that an immersion time of 15 min may not be the best time for the traditional layer-by-layer electrostatic self-assembly. After the coating immersing in dopamine solution for 1 h, the positive potential of pTi/PSP/DA was lower than that of pTi/PSP, which may attribute to dopamine nanoparticles possessing a small amount of negative

https://dx.doi.org/10.1021/acsomega.0c00986
ACS Omega 2020, 5, 10562−10571

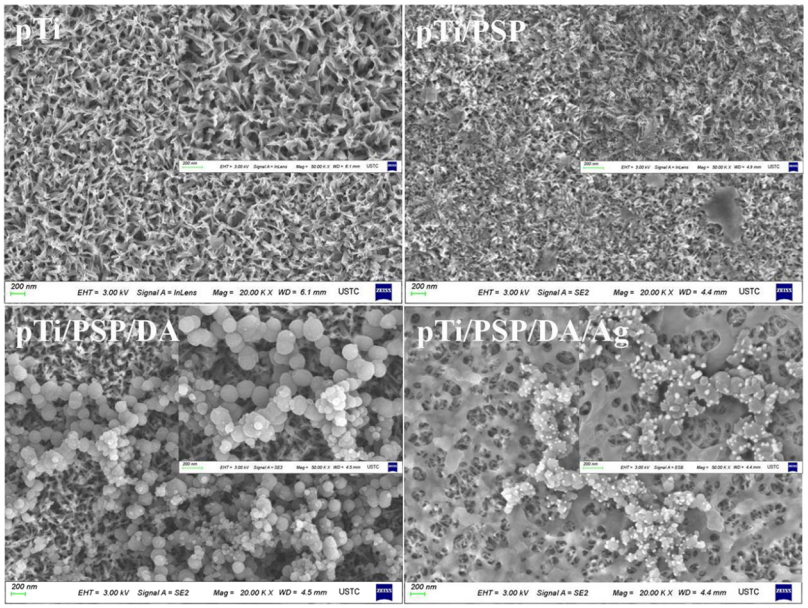

Figure 3. SEM images of pTi, pTi/PSP, pTi/PSP/DA, and pTi/PSP/DA/Ag.

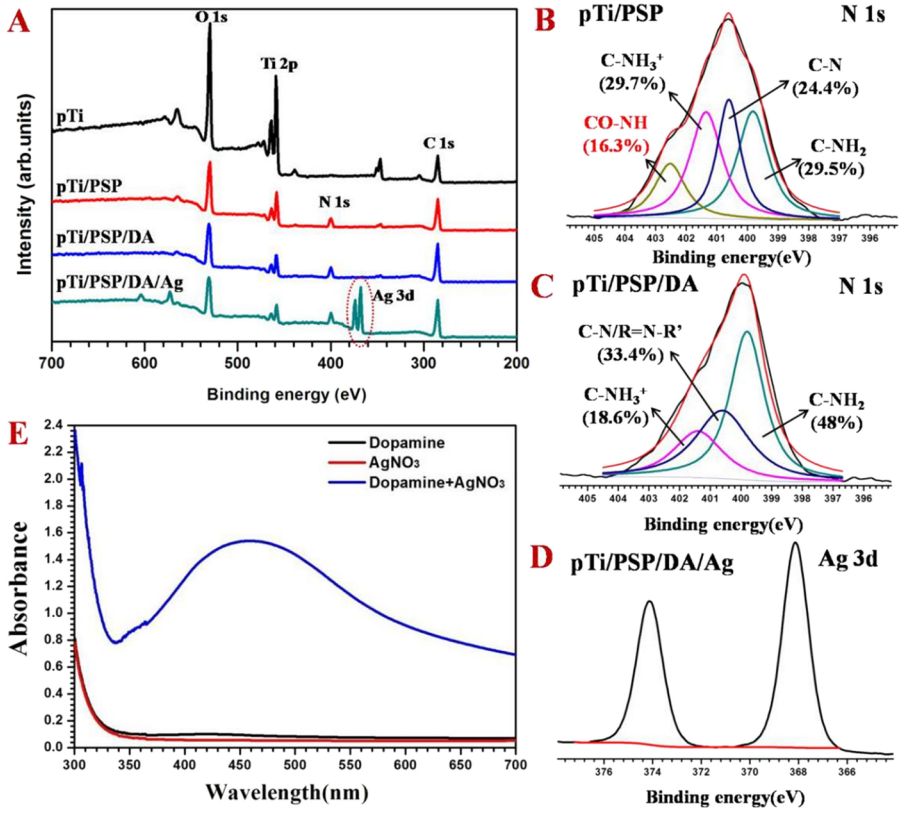

Figure 4. (A) XPS wide scans of the different surface. High resolution of N 1s of the (B) pTi/PSP and (C) pTi/PSP/DA surface. (D) High-resolution of Ag 3d of the pTi/PSP/DA/Ag coating. (E) UV−visible spectrum of different solutions.

charge (−3.25 mV; Figure 2B). In addition, the SZP value of pTi/PSP/DA/Ag became negative after the deposition of reduced AgNPs onto the pTi/PSP/DA surface, which is due to the silver nanoparticles possessing a negative charge (−22.35 mV; Figure 2C). These results provide proof that the PSP polyelectrolyte, dopamine, and silver were feasibly deposited on the alkali-heat treated titanium surfaces.

Scanning electron microscopy (SEM) was used to study the morphology of the surface after each surface modification step. As shown in Figure 3, a uniform nanoporous surface with many struts (pTi) was formed by alkali-heat treatments. After the polyelectrolyte coating build-up process, a portion of the pore space was filled, indicating that the PSP layer was successfully coated. After dopamine deposition, some spherical nanoparticles appeared on the surface of Ti/PSP, which may

https://dx.doi.org/10.1021/acsomega.0c00986
ACS Omega 2020, 5, 10562−10571

be due to the oxidation polymerization of dopamine. After AgNP deposition (pTi/PSP/DA/Ag), a large number of dopamine spheres decreased in size and formed a porous membrane-like structure on the surface due to the cross-linking reaction between dopamine spheres; meanwhile, AgNPs were distributed on the surface of dopamine spheres with a size of ~20−30 nm. Because the porous structure is important for osseointegration, the immersion time for dopamine modification was set to 1 h to prevent the formation of the blend film. Some studies indicated that antibacterial ability and cytotoxicity could be controlled by adjusting the immersion time of modified Ti in the silver solution.[34] In this study, an immersion time of 30 min for pTi/PSP/DA/Ag was used, which was expected to obtain the antibacterial ability and acceptable osteoblast compatibility with a low toxic effect. The above results demonstrated that the Ag-loaded composite coating (pTi/PSP/DA/Ag) was successfully prepared on the porous titanium surface.

To further confirm the chemical composition of different surfaces, X-ray photoelectron spectroscopy (XPS) analyses were performed. The wide scan spectra are shown in Figure 4A. The decrease in the Ti 2p peak intensity and the presence of the N 1s peak in pTi/PSP suggested that PLL and SA were successfully incorporated onto the titanium surface. The presence of the Ag 3d peak in pTi/PSP/DA/Ag suggested that silver was successfully incorporated onto the surface. To illustrate that dopamine was incorporated onto the surface, N 1s (Figure 4B,C) peak fittings were further performed. Compared to that in the high-resolution spectrum of pTi/PSP (Figure 4B), one peak in the N 1s spectrum of pTi/PSP/DA at ~402.54 eV disappeared (Figure 4C), which was consistent with the formation of CO-NH groups in the PLL, illustrating that dopamine was successfully incorporated onto the surface. The high-resolution spectrum of Ag (Figure 4D) showed two peaks and centered at the binding energies of 367.4 and 373.4 eV, attributed to Ag $3d_{5/2}$ and Ag $3d_{3/2}$, respectively, because the polydopamine with catechol and nitrogen functional groups can reduce Ag^+ to Ag^0.[35] The characteristic surface plasmon resonance (SPR) peaks of AgNPs were at λ_{max} = 400−500 nm.[36] The UV−vis spectra of dopamine, $AgNO_3$, and a mixture of dopamine and $AgNO_3$ are shown in Figure 4E. Neither dopamine nor $AgNO_3$ solution presents an absorbance peak position. However, a mixture solution of dopamine and $AgNO_3$ has a strong absorption at 450 nm, indicating that the Ag^+ in the solution was reduced to Ag^0 and formed AgNPs.[37]

Semiquantitative results of the surface chemical elemental on different surfaces are shown in Table 1. As each step of the reaction proceeded, the titanium content continued to decline, illustrating that the titanium substrate was gradually covered. Compared with that in pTi, the nitrogen contents in pTi/PSP and pTi/PSP/DA were increased because of the high proportion of nitrogen in PLL and dopamine. The presence of the Ag content confirms the successful in situ reduction of Ag onto the coating.

Table 1. Surface Chemical Elemental Composition of the Sample (atom %) was Obtained by XPS

coating	C	N	O	Ti	Ag
pTi	29.55	0.95	51.28	18.22	
pTi/PSP	49.92	7.99	32.31	9.78	
pTi/PSP/DA	56.58	9.05	29.16	5.21	
pTi/PSP/DA/Ag	56.54	8.98	26.43	3.67	4.39

Water contact angle (WCA) measurements were used to assess the wettability of different surfaces. As shown in Figure 5A, the WCA value of Ti was 80 ± 2°. Compared with that of Ti, the value for pTi decreased significantly to 5 ± 3°. After polyelectrolyte coating functionalization (pTi/PSP) and dopamine modification (pTi/PSP/DA), the contact angle increased significantly to 15 ± 2° and 21 ± 2°, respectively. The WCA of pTi/PSP/DA/Ag was 23 ± 2°, and there was no significant difference in the surface hydrophilicity between pTi/PSP/DA and pTi/PSP/DA/Ag. It is speculated that the surface with small size and low-coverage of AgNPs made the surface expose numerous dopamine, which was in agreement with the SEM results. The WCA measurements provided additional proof that the polyelectrolyte, dopamine, and AgNPs were successfully modified on the titanium surface, and the Ag-loaded surface was hydrophilic.

Silver Release. In the silver release profile of pTi/PSP/DA/Ag (Figure 5B), a sharp release of Ag from the coating occurred in the first 6 days, and then, the silver release tended to stabilize at ~2 μg every 3 days. The results showed that the cumulative release of silver in the first 6 days was equal to that in the next 21 days, and the maximum silver concentration released was far below 10 mg/L, which is toxic lever to human tissue.[38]

Mineralization of the Coating. The pTi/PSP/DA/Ag samples were incubated with simulated body fluid (SBF) for 1 week to simulate the interaction between the body fluid and sample surface during the early postoperative period. The surface morphology and composition of mineralized pTi/PSP/DA/Ag (pTi/PSP/DA/Ag-M) were obtained by SEM (Figure 5C) and energy-dispersive spectroscopy analysis (EDS) (Figure 5D). The SEM image shows the mineralized products covering the surface, which is similar to another study about dopamine inducing surface mineralization.[30] The atomic composition was analyzed using EDS and shows that the mass fractions of Ca and P were 21.9 and 12.7%, respectively, which suggested that the mineralization happened on the surface of pTi/PSP/DA/Ag. Zhang et al. reported that the dopamine-modified surface could promote mineralization[7,21] because electrostatic and coordination interactions occurred between Ca^{2+} and phenolic hydroxyl groups, further attracting PO_4^{3+} to form mineralized products. The Ca/P atomic ratio of the mineralized surface was ~1.35 and lower than the theoretical value of pure hydroxyapatite of ~1.67, indicating that the mineralized products were Ca-deficient.[39] Because the CaP mineral is an excellent bioactive material, we speculated that the cytocompatibility of pTi/PSP/DA/Ag could gradually be improved by the surface mineralization during the early postoperative period.

Antibacterial Property. Biomaterial-related infections caused by bacterioplankton around the implant and adherent bacteria on the implant surface commonly lead to implant failures and even alveolar bone loss. Owing to the broad spectrum bactericidal ability of Ag, the Ag-loaded coating was expected to present vigorous antibacterial activity. The reduced AgNPs could be released into the medium in the form of Ag^+ to destroy bacteria and prevent bacteria proliferation. The zone of inhibition (ZOI) test was used to assess the inhibitory ability of the surface toward *Streptococcus mutans* (*S. mutans*) and *Staphylococcus aureus* (*S. aureus*) around samples. As shown in Figure 6A, the results showed that the pTi/PSP/DA/

https://dx.doi.org/10.1021/acsomega.0c00986
ACS Omega 2020, 5, 10562−10571

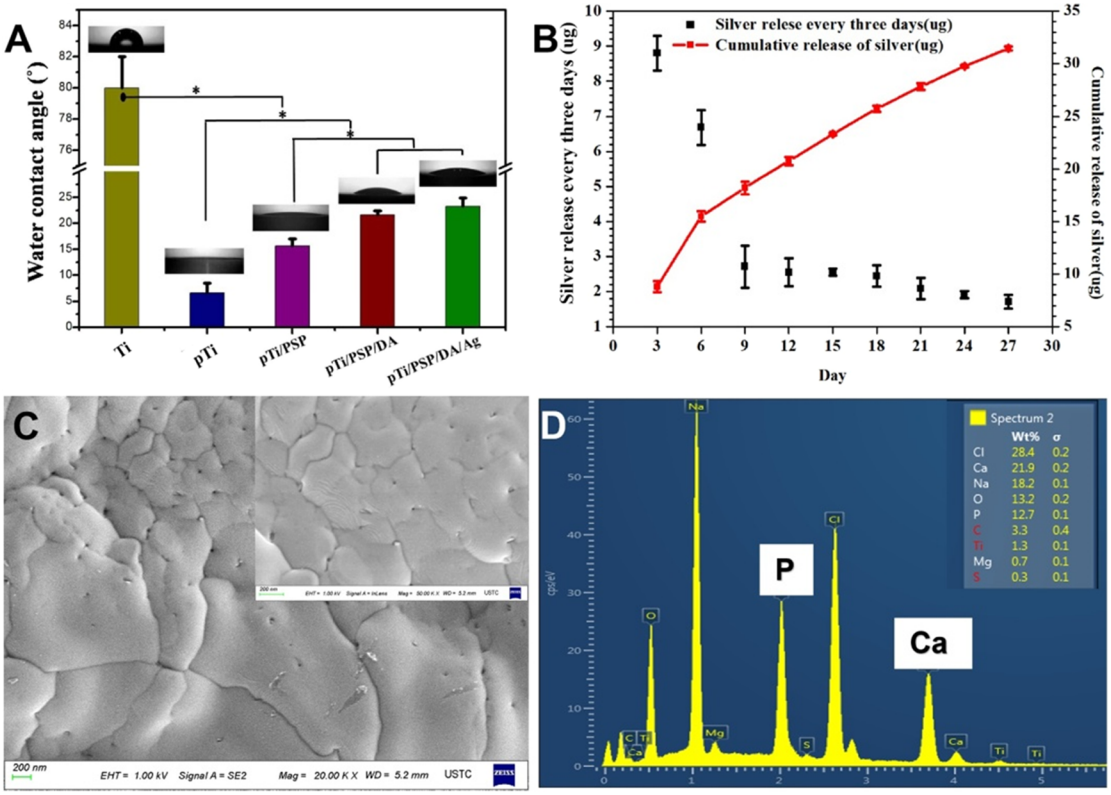

Figure 5. (A) WCAs of different surfaces. (B) The silver mass was released into PBS every 3 days, and the cumulative release into PBS was sustained for 27 days. (C) SEM image and (D) EDS spectra of the mineralized surface of pTi/PSP/DA/Ag (pTi/PSP/DA/Ag-M).

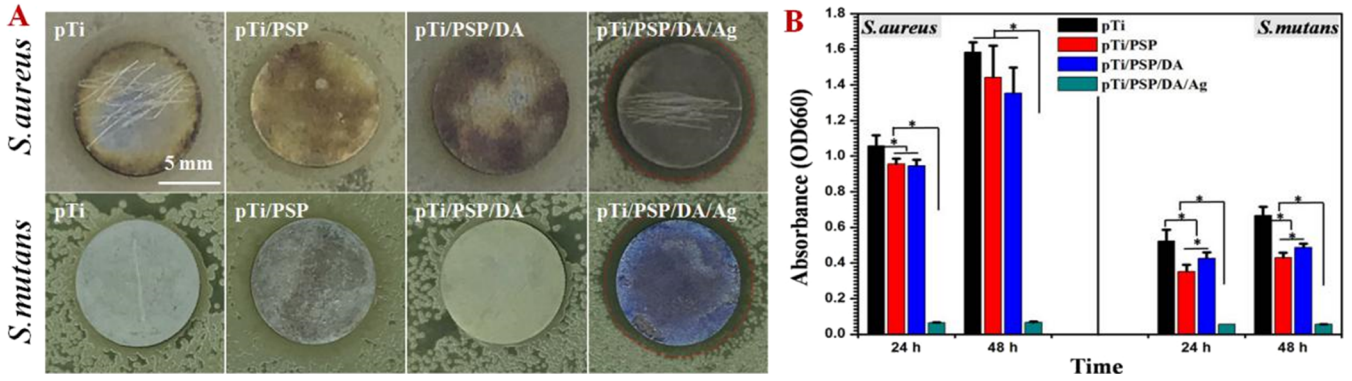

Figure 6. ZOI tests of different samples against (A) *S. aureus* and *S. mutans* and (B) histogram of bacterial proliferation.

Ag surface exhibited a clear ring (no bacteria around the sample), indicating that AgNPs inhibited growth or killed bacteria around them. To monitor the growth of the bacteria incubated with the sample in the medium, the optical density was measured using a microplate reader at 660 nm, as shown in Figure 6B. Because the optical density (OD) value was positively correlated with the number of bacteria in the suspension, this result showed that only the Ag-loaded coating could completely inhibit proliferation of *S. aureus* and *S. mutans* after 24 and 48 h of incubation. These two methods are used to prove that the pTi/PSP/DA/Ag surface inhibits the growth of bacteria around them.

Because bacteria adhering on the surface of an implant are key factors leading to biomaterial-associated infections, functional modification can inhibit the adhesion of bacteria on the surface. Therefore, two methods were used to observe the number of bacteria on different surfaces. (i) A commercially available kit for live/dead bacteria staining was utilized to evaluate the viability of bacteria in situ after 24 h of cultivation. Figure 7A shows that massive numbers of bacteria adhered to pTi, pTi/PSP, and pTi/PSP/DA; meanwhile, few bacteria adhered to pTi/PSP/DA/Ag, and the number of dead cells (red) was higher than that of live cells (green) on pTi/PSP/DA/Ag, indicating that silver could restrain bacterial adhesion and kill adherent bacteria. (ii) After 24 h of cultivation, bacteria adhered on each surface of the samples were dispersed in phosphate-buffered saline (PBS) solution and then recultured on agar plates to indirectly observe the number of live bacteria on the modified Ti surface. As shown in Figure 7B, many bacterial colonies were observed on the surface of pTi, pTi/PSP, and pTi/PSP/DA, but no bacterial colonies were found on pTi/PSP/DA/Ag. The above results verified that the silver-modified surface could inhibit bacterial adhesion and kill the adherent bacteria.

https://dx.doi.org/10.1021/acsomega.0c00986
ACS Omega 2020, 5, 10562−10571

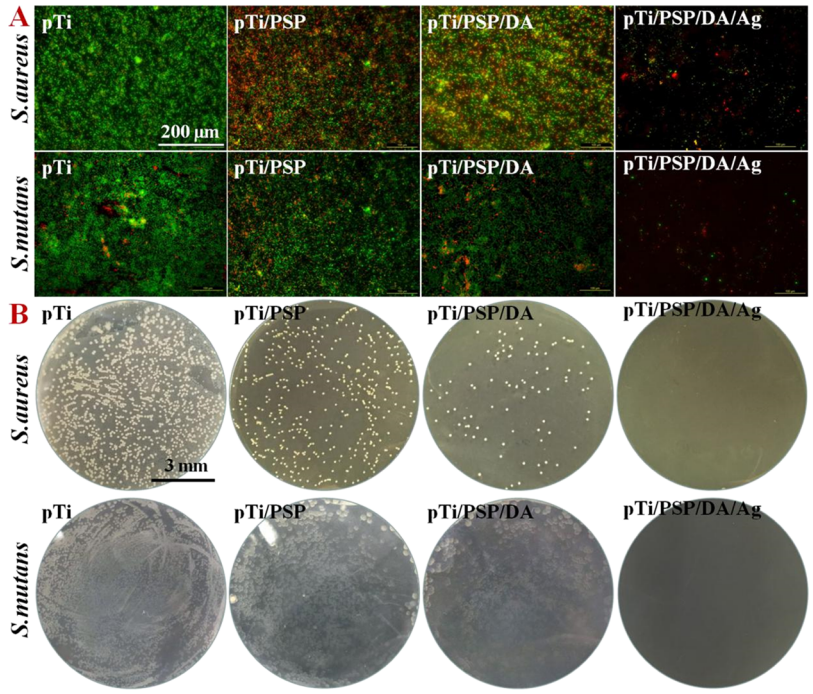

Figure 7. (A) Fluorescence micrographs of *S. aureus* and *S. mutans* on different surfaces after incubation for 24 h, visualizing live (green) and dead (red) cells. (B) Bacterial CFUs on different surfaces.

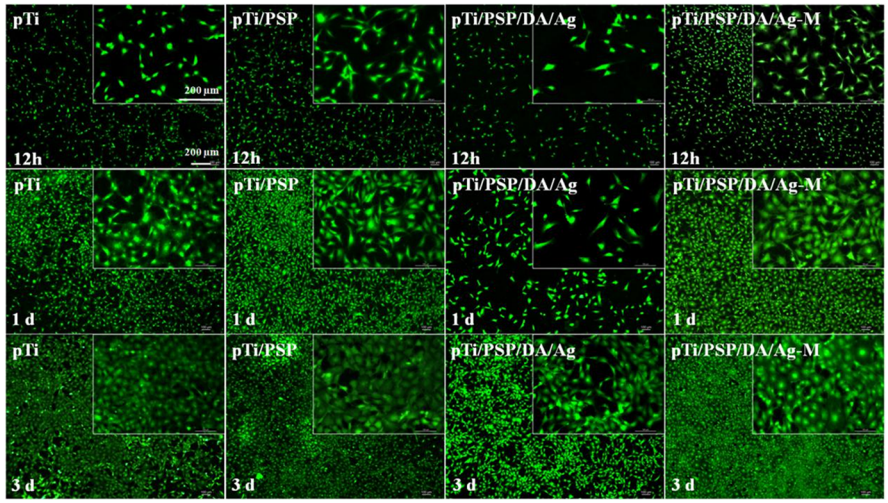

Figure 8. Fluorescence images of live cells cultured on the modified samples after 12 h, 1 day, and 3 days.

In dentistry, periodontitis or peri-implantation inflammation caused by bacterial infection may cause tooth/implant loss.[40,41] During dental implant placement, bacterial adhesion and biofilm formation are difficult to remove by systemic antibiotics.[42] Then, the bacteria can invade the bloodstream and lead to underlying life-threatening general infections, tissue damage, and even infective endocarditis.[43] Therefore, there are many antibacterial strategies to avoid biofilm formation by preventing bacterial adhesion or killing them in the early stage. The antibacterial results showed that the pTi/PSP/DA/Ag surface inhibited bacterial adhesion and killed adherent bacteria on the surface to reduce the risk of pathogen colonization on the implant surface; meanwhile, bacteria around the implant were killed by the released silver (Figure 5B) to prevent bacterial infection from the surrounding soft tissue. The antibacterial activity could protect the implant in the early postoperative period.[44]

Cytocompatibility Assessment. The facile method provides a stable antibacterial coating with controllable Ag release for preventing infection; then, the cytotoxicity of the surface needs to test. Osteoblasts have an important impact on bone modeling and remodeling; thus, we investigated whether the coating could affect mouse osteoblast-like cell line (MC3T3-E1) adhesion and proliferation via fluorescence staining of cells and MTT assay.

Figure 8 shows the adherent osteoblasts on various samples through cytoskeletal actin staining by rhodamine 123 after seeding for 12 h, 1 day, and 3 days. The total number and morphology of cells on the different surfaces were observed. More cells adhered to the pTi/PSP surface than to the pTi surface, indicating that the porous structure with polyelec-

https://dx.doi.org/10.1021/acsomega.0c00986
ACS Omega 2020, 5, 10562−10571

trolyte coating-favored cell adhesion. The number and size of osteoblasts adhered to the pTi/PSP/DA/Ag surface was obviously less than to the other surfaces due to the cytotoxicity of AgNPs. However, the adherent cells on the surface of pTi/PSP/DA/Ag exhibited good spread and most surfaces of that were covered by cells after culturing for 3 days. Meanwhile, the mineralized surface (pTi/PSP/DA/Ag-M) exhibited good osteoblast compatibility because the number of adherent osteoblasts on this surface was more than that on the pTi surface. After culturing for 3 days, the morphology of the adherent cells on these surfaces exhibited active polygonal and pseudopodia-like structures, indicating that the cells maintained good cellular activity.

The MTT assay was performed to assess cell proliferation of MC3T3-E1 on different surfaces and is shown in Figure 9.

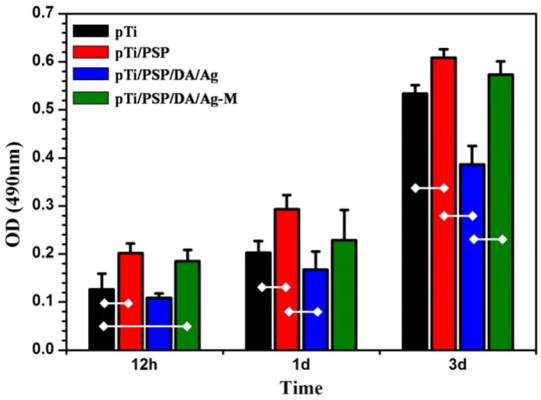

Figure 9. MTT viability test of MC3T3-E1 cells cultured for 12 h, 1 day, and 3 days.

Compared with other groups, the surface of the pTi/PSP exhibited higher cell viability, which suggested that polyelectrolyte coating was beneficial to cell adhesion and proliferation. After AgNP modification, the viability of cells significantly decreased, indicating that the pTi/PSP/DA/Ag surface had a cytotoxic effect. However, the mineralized surface (pTi/PSP/DA/Ag-M) exhibited a significantly higher cell proliferation rate than the pTi, which was in agreement with the results of fluorescence staining.

Taken together, the above results indicated that the polyelectrolyte coating (pTi/PSP) exhibited excellent cellular activity for cell adhesion and proliferation. Though pTi/PSP/DA/Ag did not initially support cell adhesion, the AgNPs did not cause severe cytotoxicity due to the significant cell proliferation on this surface. It is speculated that the Ag-loaded amount was at a low level. In addition, the mineralized pTi/PSP/DA/Ag coating could greatly enhance the cytocompatibility.

The main cause of implant failure is peri-implant inflammation associated with bacterial invasion, which then results in bone absorption around the implant and ultimately leads to loosening of the implant. The purpose of the modification surface is to make the material antibacterial and cytocompatibility property. Antibacterial properties take priority. The AgNP-modified surface could protect the implant from bacterial infection, while the balance between antibacterial activity and cytocompatibility needs to be considered due to the cytotoxicity of silver.

The hydrophilic surface is advantageous for cell adhesion and proliferation, which impacts the first stage of initial osseointegration.[45] Here, excellent hydrophilicity of the surfaces of pTi, pTi/PSP, pTi/PSP/DA, and pTi/PSP/DA/Ag (Figure 5A) was obtained. Through electrostatic assembly, the surface cytocompatibility of pTi/PSP was better than that of pTi, presumably because there were many amino groups in PLL, which could electrostatically interact with the cell membrane (negative charge).[46] In addition, the polyelectrolyte coating did not cover the porous structure, which increased the surface area and benefited cell adhesion. Dopamine nanoparticles were combined onto the polyelectrolyte coating and formed porous film and reduced Ag ions to form AgNPs. The results of osteoblast compatibility showed that the coating of pTi/PSP/DA/Ag did not support osteoblast adhesion at first due to the toxicity of silver, but it did not inhibit the cell proliferation, which suggested that the Ag-loaded amount on the surface was at a safe level. Furthermore, when pTi/PSP/DA/Ag was immersed in SBF for 7 days, mineralization happened by inducing a mineral from SBF to deposition on the surface and then greatly improving osteoblast compatibility.

CONCLUSIONS

The composite coating of polyelectrolyte, dopamine, and AgNPs was successfully prepared on a porous titanium surface. AgNPs with sizes of 20−30 nm were bound onto dopamine particles. The release of Ag lasted for at least 27 days. After incubation with *S. aureus* and *S. mutans*, pTi/PSP/DA/Ag could prevent bacterial adhesion and colonization. The composite coating had mild cytotoxicity to prevent cell adhesion, but this coating could induce mineralization on the surface when incubated in SBF and then exhibited good cytocompatibility. Thus, we concluded that the silver-loaded coating could prevent bacterial infections and facilitate mineralization *in vivo* in the early postoperative period, and then, the mineralized surface exhibit good cytocompatibility. This design could be a potentially valuable application for antibacterial dental- and orthopedic-related applications.

MATERIALS AND METHODS

Materials. Commercial pure Ti plates (10 mm × 10 mm × 2 mm) were purchased from Baoji Nonferrous Metal Co., Ltd. (Shanxi province, China). Sodium alginate (SA), ε-poly-L-lysine (PLL) (MW < 5000), dopamine (DA), Tris−HCl, and silver nitrate were purchased from Sigma-Aldrich. Trypsin−EDTA solution, α-minimum Eagles medium (α-MEM) for cells culture, penicillin and streptomycin, and fetal bovine serum (FBS) were purchased from Gibco.

Fabrication of the Composite Coating. Titanium plates were polished with SiC abrasive papers in the order of increasing grid (600, 800, 1000, 1200, 1500, and 2000 grit) and cleaned ultrasonically for 15 min in successive baths in acetone, anhydrous ethanol, and deionized water. Ti plates were immersed in 2.5 M NaOH solution at 60 °C for 12 h to form a porous surface and were denoted as pTi. The pTi samples were in turn immersed in the 5 mg/mL PLL solution, 5 mg/mL SA solution, and 5 mg/mL PLL solution for 12 h each; after every polyelectrolyte adsorption steps, the samples were rinsed with deionized water and were labeled as pTi/PSP. Then, the samples of pTi/PSP were immersed in an aqueous solution containing 1 mg/mL dopamine and 1.5 mg/mL Tris buffer for 1 h to form dopamine coating and were marked as pTi/PSP/DA. Finally, samples of pTi/PSP/DA were im-

https://dx.doi.org/10.1021/acsomega.0c00986
ACS Omega 2020, 5, 10562−10571

mersed in silver nitrate solution (AgNO3, 4 mg/mL) for 30 min to form AgNPs and were denoted as pTi/PSP/DA/Ag.

Surface Characterization. The surface zeta potentials (SZP) of different samples were obtained by a zeta potential analyzer coupled with a surface zeta potential electrode (NanoBrook-90Pus PALS, Brookhaven, USA). Instead of Ti plates, titanium foils (7 mm × 4 mm × 0.2 mm) were used to adapt to shapes of an electrode in potential measurements. After different treatments, the titanium foils were attached a sample holder via a double-sided adhesive tape and then were immersed in a standard solution with 0.025 mg/mL BI-ZR51 and 1 mM KCl (pH = 7, 37 °C). By measuring the zeta potentials of the standard solution at a range of known distances from the sample surface, a linear relationship between zeta potential and distances was built and the SZPs of different surfaces were obtained based on the linear relationship at a distance of zero. Besides, polydopamine nanoparticles and AgNPs were collected separately by centrifugation from the aqueous solution containing dopamine (1 mg/mL)/Tris buffer (1.5 mg/mL) and silver nitrate solution ($AgNO_3$, 4 mg/mL) and then were dispersed in deionized water (pH = 7) by the ultrasonic processing. Then, the zeta potentials of polydopamine nanoparticles and AgNPs were determined by the zeta potential analyzer.

The morphologies of the surface-modified samples were observed through scanning electron microscopy (SEM; Hitachi S-4800).

Elemental compositions were characterized by an XPS (Thermo ESCALAB 250) instrument equipped with an Al Kα X-ray source (1486.6 eV photons) that was utilized to analyze data at a pass energy of 100 eV; at the same time, high-resolution scans of 30 eV pass-through energy were utilized to obtain detailed component compositions. The C 1s peak at 284.8 eV was used to calibrate the system. In this process, the investigation depth was limited to 10 nm by setting the takeoff angle to 45°. Quantitative analysis and XPS spectra were fitted using the XPS peak software.

The water contact angle (WCA) was measured by using deionized water in a contact angle measurement machine (Chenghui JGW-360A China) at room temperature. The absorption of ultraviolet−visible light was measured by a UV−vis spectrophotometer (Shimadzu TU-1800 Japan).

Mineralization of the Coating. To study the mineralization performance of the as-prepared surface, samples of pTi/PSP/DA/Ag were incubated in 2 mL of simulated body fluid (SBF; pH = 7.5). The samples were placed in a shaker incubator at 37 °C with 100 rpm, and the SBF was changed daily. After incubating for 7 days, these samples were removed and rinsed heavily with deionized water for 10 min and denoted as pTi/PSP/DA/Ag-M. The morphology and chemical element composition of the samples surfaces were investigated by SEM and energy-dispersive spectroscopy (EDS), respectively.

Silver Release. To study the release capacity and release profile of silver from the Ag-loaded coating, pTi/PSP/DA/Ag was immersed in 2 mL of PBS solution on an orbital shaker at 37 °C for up to 27 days. The solution was collected at different periods (i.e., on days 3, 6, 9, 12, 15, 18, 21, and 27) and replaced with a fresh PBS solution. The concentration of released Ag was tested by inductively coupled plasma atomic emission spectrometry (ICP-AES Perkin-Elmer Corporation Optima 7300 DV).

Antimicrobial Test. The antibacterial properties of the samples were evaluated using two oral microbes, including *S. mutans* and *S. aureus*. Bacteria were cultivated in the BHI medium at 37 °C overnight in an incubator. The bacterial suspension was diluted to achieve a final concentration of 10^6 CFU/mL.

The zone of inhibition (ZOI) was used to determine the bacteriostatic effect of the sample on bacteria. The solid medium agar plate surface was spread with 70 μL of bacterial suspensions, and the sample to be tested was placed face down on the agar plate and then incubated for 24 h at 37 °C. In addition, samples were incubated in 2 mL of bacterial suspensions at 37 °C. After 24 and 48 h of incubation, 150 μL of bacterial suspension was removed for optical density measurements at 660 nm (OD660) using a microplate reader (Bio-tek MQX200). The method was assessed as an inhibition of the local bacterium growth around the modified Ti.

The bactericidal ability of different samples was observed using the CFU counting method and live/dead bacteria assay. The samples were incubated in 2 mL of bacterial suspensions at 37 °C. After incubation for 24 h, (i) each sample was removed and ultrasonic and vortex processing were performed with PBS. Then, microliters of the PBS solution was diluted 1000-fold with PBS. Then, 100 μL aliquots were recultured on agar plates to count CFUs at 37 °C for 24 h. (ii) The sample was rinsed gently with PBS to remove unattached bacteria, stained with the LIVE/DEAD BacLight Bacterial Viability Kit (Invitrogen, Carlsbad, CA) for 10 min in a dark room, and observed using a fluorescence inverted microscope (Leica, Germany).

Cell Culture and Cytocompatibility Assessment. To evaluate cytocompatibility, the mouse osteoblast cells were cultured at 37 °C and a 5% CO_2 incubator in α-MEM supplemented with 10% FBS and 1% penicillin−streptomycin. The culture medium was changed every 2 days.

Cells were seeded with at a density of 1×10^5 cells/mL on the surface of the sample in a 24-well plate. After incubating with the sample for 12 h, 24 h and 3 days, 40 μL of the MTT reagent was added to each well and reacted for 3 h. Samples were removed and placed in a new 24-well plate, 200 μL of DMSO solutions was added to each well followed by reaction for 10 min, 150 μL of mixed solution was transferred to a 96-well plate, and the absorbance was detected using a microplate reader (Bio-tek MQX200) at 490 nm. In addition, at each point in time, another sample of every group were removed and rinsed with PBS. The cells were fixed with 1% glutaraldehyde for 2 h. Then, rhodamine 123 was used to stain the cells for 10 min in the dark, and then, samples were observed with a fluorescence microscope.

Statistics. The data represent the mean ± standard deviation (n = 3) and were assessed by one-way analysis of variance (ANOVA) for the determination of significant differences between test groups. Statistical differences were marked as asterisks (*) for mean statistically significance set at $p < 0.05$ in the figures.

Ethical Statement. All experimental protocols used in this research were approved by the Ethical Committee of Anhui Medical University (protocol number: 20160126).

AUTHOR INFORMATION

Corresponding Author

Jialong Chen − *Stomatologic Hospital and College, Key Laboratory of Oral Diseases Research of Anhui Province, Anhui*

https://dx.doi.org/10.1021/acsomega.0c00986
ACS Omega 2020, 5, 10562−10571

Medical University, Hefei, Anhui 230032, China; orcid.org/0000-0002-5323-1801; Phone: +8613721090114; Email: jialong_dt@126.com; Fax: +86-551-65161183

Authors

Chuchu Guo − *Stomatologic Hospital and College, Key Laboratory of Oral Diseases Research of Anhui Province, Anhui Medical University, Hefei, Anhui 230032, China*

Wendi Cui − *Stomatologic Hospital and College, Key Laboratory of Oral Diseases Research of Anhui Province, Anhui Medical University, Hefei, Anhui 230032, China*

Xiaowei Wang − *Stomatologic Hospital and College, Key Laboratory of Oral Diseases Research of Anhui Province, Anhui Medical University, Hefei, Anhui 230032, China*

Xiaoxuan Lu − *Stomatologic Hospital and College, Key Laboratory of Oral Diseases Research of Anhui Province, Anhui Medical University, Hefei, Anhui 230032, China*

Lulu Zhang − *Stomatologic Hospital and College, Key Laboratory of Oral Diseases Research of Anhui Province, Anhui Medical University, Hefei, Anhui 230032, China*

Xiangyang Li − *Stomatologic Hospital and College, Key Laboratory of Oral Diseases Research of Anhui Province, Anhui Medical University, Hefei, Anhui 230032, China*

Wei Li − *Stomatologic Hospital and College, Key Laboratory of Oral Diseases Research of Anhui Province, Anhui Medical University, Hefei, Anhui 230032, China*

Weibo Zhang − *Stomatologic Hospital and College, Key Laboratory of Oral Diseases Research of Anhui Province, Anhui Medical University, Hefei, Anhui 230032, China*

Complete contact information is available at: https://pubs.acs.org/10.1021/acsomega.0c00986

Author Contributions

†C.G., W.C., and X.W. contributed equally to this work.

Notes

The authors declare no competing financial interest.

■ ACKNOWLEDGMENTS

This work was supported by the National Natural Science Foundation of China (no. 31670967), the Scientific Research Foundation of the Institute for Translational Medicine of Anhui Province (no. 2017zhyx19), the University Outstanding Youth Talent Support Program of Anhui Province (no.gxyq2018007), and the Postdoctoral Science Foundation of Anhui Province (no. 2018B264).

■ REFERENCES

(1) Elahinia, M. H.; Hashemi, M.; Tabesh, M.; Bhaduri, S. B. Manufacturing and processing of NiTi implants: A review. *Prog. Mater. Sci.* **2012**, *57*, 911−946.

(2) Kutty, M. G.; De, A.; Bhaduri, S. B.; Yaghoubi, A. Microwave-Assisted Fabrication of Titanium Implants with Controlled Surface Topography for Rapid Bone Healing. *ACS Appl. Mater. Interfaces* **2014**, *6*, 13587−13593.

(3) Mohseni, E.; Zalnezhad, E.; Bushroa, A. R. Comparative investigation on the adhesion of hydroxyapatite coating on Ti−6Al−4V implant: A review paper. *Int. J. Adhes. Adhes.* **2014**, *48*, 238−257.

(4) De Avila, E. D.; Lima, B. P.; Sekiya, T.; Torii, Y.; Ogawa, T.; Shi, W.; Lux, R. Effect of UV-photofunctionalization on oral bacterial attachment and biofilm formation to titanium implant material. *Biomaterials* **2015**, *67*, 84−92.

(5) Butev, E.; Esen, Z.; Bor, S. In vitro bioactivity investigation of alkali treated Ti6Al7Nb alloy foams. *Appl. Surf. Sci.* **2015**, *327*, 437−443.

(6) Shao, S.-y.; Ming, P.-p.; Qiu, J.; Yu, Y.-j.; Yang, J.; Chen, J.-x.; Tang, C.-b. Modification of a SLA titanium surface with calcium-containing nanosheets and its effects on osteoblast behavior. *RSC Adv.* **2017**, *7*, 6753−6761.

(7) Zhang, W.; Wang, S.; Ge, S.; Chen, J.; Ji, P. The relationship between substrate morphology and biological performances of nano-silver-loaded dopamine coatings on titanium surfaces. *R. Soc. Open Sci.* **2018**, *5*, 172310.

(8) Li, L.; Gao, J.; Wang, Y. Evaluation of cyto-toxicity and corrosion behavior of alkali-heat-treated magnesium in simulated body fluid. *Surf. Coat. Technol.* **2004**, *185*, 92−98.

(9) Cooper, T. M.; Campbell, A. L.; Crane, R. L. Formation of polypeptide-dye multilayers by electrostatic self-assembly technique. *Langmuir* **1995**, *11*, 2713−2718.

(10) Carrillo, J. M. Y.; Dobrynin, A. V. Layer-by-Layer Assembly of Charged Nanoparticles on Porous Substrates: Molecular Dynamics Simulations. *ACS Nano* **2011**, *5*, 3010−3019.

(11) Shi, Q.; Qian, Z.; Liu, D.; Liu, H. Surface Modification of Dental Titanium Implant by Layer-by-Layer Electrostatic Self-Assembly. *Front. Physiol.* **2017**, *8*, 574.

(12) Cai, K.; Hu, Y.; Jandt, K. D.; Wang, Y. Surface modification of titanium thin film with chitosan via electrostatic self-assembly technique and its influence on osteoblast growth behavior. *J. Mater. Sci.-Mater Med.* **2008**, *19*, 499−506.

(13) Chen, J. L.; Li, Q. L.; Chen, J. Y.; Chen, C.; Huang, N. Improving blood-compatibility of titanium by coating collagen−heparin multilayers. *Appl. Surf. Sci.* **2009**, *255*, 6894−6900.

(14) Chen, J.; Chen, C.; Chen, Z.; Chen, J.; Li, Q.; Huang, N. Collagen/heparin coating on titanium surface improves the biocompatibility of titanium applied as a blood-contacting biomaterial. *J. Biomed. Mater. Res., Part A.* **2010**, *95A*, 341−349.

(15) Chen, J.; Huang, N.; Li, Q.; Chu, C. H.; Li, J.; Maitz, M. F. The effect of electrostatic heparin/collagen layer-by-layer coating degradation on the biocompatibility. *Appl. Surf. Sci.* **2016**, *362*, 281−289.

(16) Daud, N. M.; Bahri, I. F. S.; Malek, N. A. N. N.; Hermawan, H.; Saidin, S. Immobilization of antibacterial chlorhexidine on stainless steel using crosslinking polydopamine film: Towards infection resistant medical devices. *Colloids Surf., B* **2016**, *145*, 130−139.

(17) Park, S.-E.; Ko, W.-K.; Park, J. H.; Bayome, M.; Park, J.; Heo, D. N.; Lee, S. J.; Moon, J.-H.; Kwon, I. K. Antibacterial Effect of Silver and Gold Nanoparticle Coated Modified C-Palatal Plate. *J. Nanosci. Nanotechnol.* **2016**, *16*, 8809−8813.

(18) Raffi, M.; Mehrwan, S.; Bhatti, T. M.; Akhter, J. I.; Hameed, A.; Yawar, W.; Hasan, M. M. Investigations into the antibacterial behavior of copper nanoparticles against Escherichia coli. *Ann. Microbiol.* **2010**, *60*, 75−80.

(19) He, T.; Zhu, W.; Wang, X.; Yu, P.; Wang, S.; Tan, G.; Ning, C. Polydopamine assisted immobilisation of copper(II) on titanium for antibacterial applications. *Mater. Technol.* **2015**, *30*, B68−B72.

(20) Jia, Z.; Xiu, P.; Li, M.; Xu, X.; Shi, Y.; Cheng, Y.; Wei, S.; Zheng, Y.; Xi, T.; Cai, H.; Liu, Z. Bioinspired anchoring AgNPs onto micro-nanoporous TiO2 orthopedic coatings: Trap-killing of bacteria, surface-regulated osteoblast functions and host responses. *Biomaterials* **2016**, *75*, 203−222.

(21) Chen, J.; Mei, M. L.; Li, Q. L.; Chu, C. H. Mussel-inspired silver-nanoparticle coating on porous titanium surfaces to promote mineralization. *RSC Adv.* **2016**, *6*, 104025−104035.

(22) Zhou, W.; Jia, Z.; Xiong, P.; Yan, J.; Li, Y.; Li, M.; Cheng, Y.; Zheng, Y. Bioinspired and Biomimetic AgNPs/Gentamicin-Embedded Silk Fibroin Coatings for Robust Antibacterial and Osteogenetic Applications. *ACS Appl. Mater. Interfaces* **2017**, *9*, 25830−25846.

(23) Fan, X.; Yang, F.; Nie, C.; Yang, Y.; Ji, H.; He, C.; Cheng, C.; Zhao, C. Mussel-Inspired Synthesis of NIR-Responsive and Biocompatible Ag-Graphene 2D Nano-Agents for Versatile Bacterial Disinfections. *ACS Appl. Mater. Interfaces* **2018**, *10*, 296−307.

(24) Meng, F.; Sun, Z. A mechanism for enhanced hydrophilicity of silver nanoparticles modified TiO_2 thin films deposited by RF magnetron sputtering. *Appl. Surf. Sci.* **2009**, *255*, 6715−6720.

(25) Azlin-Hasim, S.; Cruz-Romero, M. C.; Cummins, E.; Kerry, J. P.; Morris, M. A. The potential use of a layer-by-layer strategy to develop LDPE antimicrobial films coated with silver nanoparticles for packaging applications. *J. Colloid Interface Sci.* **2016**, *461*, 239−248.
(26) Jin, G.; Qin, H.; Cao, H.; Qian, S.; Zhao, Y.; Peng, X.; Zhang, X.; Liu, X.; Chu, P. K. Synergistic effects of dual Zn/Ag ion implantation in osteogenic activity and antibacterial ability of titanium. *Biomaterials* **2014**, *35*, 7699−7713.
(27) Liu, Y.; Ai, K.; Lu, L. Polydopamine and Its Derivative Materials: Synthesis and Promising Applications in Energy, Environmental, and Biomedical Fields. *Chem. Rev.* **2014**, *114*, 5057−5115.
(28) Li, X.; Liu, J.; Yang, T.; Qiu, H.; Lu, L.; Tu, Q.; Xiong, K.; Huang, N.; Yang, Z. Mussel-inspired "built-up" surface chemistry for combining nitric oxide catalytic and vascular cell selective properties. *Biomaterials* **2020**, *241*, 119904.
(29) Zhang, F.; Zhang, Q.; Li, X.; Huang, N.; Zhao, X.; Yang, Z. Mussel-inspired dopamine-CuII coatings for sustained in situ generation of nitric oxide for prevention of stent thrombosis and restenosis. *Biomaterials* **2019**, *194*, 117−129.
(30) Li, M.; Liu, X.; Xu, Z.; Yeung, K. W. K.; Wu, S. Dopamine Modified Organic−Inorganic Hybrid Coating for Antimicrobial and Osteogenesis. *ACS Appl. Mater. Interfaces* **2016**, *8*, 33972−33981.
(31) Orive, G.; Tam, S. K.; Pedraz, J. L.; Hallé, J.-P. Biocompatibility of alginate−poly-l-lysine microcapsules for cell therapy. *Biomaterials* **2006**, *27*, 3691−3700.
(32) Montalbano, G.; Toumpaniari, S.; Popov, A.; Duan, P.; Chen, J.; Dalgarno, K.; Scott, W. E., III; Ferreira, A. M. Synthesis of bioinspired collagen/alginate/fibrin based hydrogels for soft tissue engineering. *Mater. Sci. Eng. C* **2018**, *91*, 236−246.
(33) Lacerda, L.; Parize, A. L.; Fávere, V.; Laranjeira, M. C. M.; Stulzer, H. K. Development and evaluation of pH-sensitive sodium alginate/chitosan microparticles containing the antituberculosis drug rifampicin. *Mat. Sci. Eng. C.* **2014**, *39*, 161−167.
(34) Rong, X.; Zhang, Y.; Tan, G. X.; Tan, Y.; Ning, C.; Li, M. The Influence of Reaction Time on the Biocompatibility of Polydopamine/Silver Nanoparticles Modified Porous Titanium. *J. Tissue Eng. Reconstr. Surg.* **2015**, *5*, 295−300.
(35) Luo, H.; Gu, C.; Zheng, W.; Dai, F.; Wang, X.; Zheng, Z. Facile synthesis of novel size-controlled antibacterial hybrid spheres using silver nanoparticles loaded with poly-dopamine spheres. *RSC Adv.* **2015**, *5*, 13470−13477.
(36) Sherry, L. J.; Chang, S.-H.; Schatz, G. C.; Van Duyne, R. P.; Wiley, B. J.; Xia, Y. Localized Surface Plasmon Resonance Spectroscopy of Single Silver Nanocubes. *Nano Lett.* **2005**, *5*, 2034−2038.
(37) Gebru, H.; Cui, S.; Li, Z.; Wang, X.; Pan, X.; Liu, J.; Guo, K. Facile pH-Dependent Synthesis and Characterization of Catechol Stabilized Silver Nanoparticles for Catalytic Reduction of 4-Nitrophenol. *Catal. Lett.* **2017**, *147*, 2134−2143.
(38) Wang, J.; Li, Z.; Liang, Y.; Zhu, S.; Cui, Z.; Bao, H.; Liu, Y.; Yang, X. Cytotoxicity and antibacterial efficacy of silver nanoparticles deposited onto Dopamine-Functionalised titanium. *Mater. Express.* **2015**, *5*, 191−200.
(39) Cheng, D.; Liu, D.; Tang, T.; Zhang, X.; Jia, X.; Cai, Q.; Yang, X. Effects of Ca/P molar ratios on regulating biological functions of hybridized carbon nanofibers containing bioactive glass nanoparticles. *Biomed. Mater.* **2017**, *12*, No. 025019.
(40) Norowski, P. A., Jr.; Bumgardner, J. D. Biomaterial and antibiotic strategies for peri-implantitis: A review. *J. Biomed. Mater. Res. Part B.* **2009**, *88B*, 530−543.
(41) Jin, J.; Zhang, L.; Shi, M.; Zhang, Y.; Wang, Q. Ti-GO-Ag nanocomposite: the effect of content level on the antimicrobial activity and cytotoxicity. *Int. J. Nanomedicine.* **2017**, *Volume 12*, 4209−4224.
(42) Gittens, R. A.; Scheideler, L.; Rupp, F.; Hyzy, S. L.; Geis-Gerstorfer, J.; Schwartz, Z.; Boyan, B. D. A review on the wettability of dental implant surfaces II: Biological and clinical aspects. *Acta Biomater.* **2014**, *10*, 2907−2918.
(43) Kerrigan, S. W.; Cox, D. Platelet−bacterial interactions. *Cell. Mol. Life Sci.* **2010**, *67*, 513−523.
(44) Cometa, S.; Bonifacio, M. A.; Baruzzi, F.; de Candia, S.; Giangregorio, M. M.; Giannossa, L. C.; Dicarlo, M.; Mattioli-Belmonte, M.; Sabbatini, L.; De Giglio, E. Silver-loaded chitosan coating as an integrated approach to face titanium implant-associated infections: analytical characterization and biological activity. *Anal. Bioanal. Chem.* **2017**, *409*, 7211−7221.
(45) Elias, C. N.; Oshida, Y.; Lima, J. H. C.; Muller, C. A. Relationship between surface properties (roughness, wettability and morphology) of titanium and dental implant removal torque. *J. Mech. Behav. Biomed. Mater.* **2008**, *1*, 234−242.
(46) Varoni, E.; Canciani, E.; Palazzo, B.; Varasano, V.; Chevallier, P.; Petrizzi, L.; Dellavia, C.; Mantovani, D.; Rimondini, L. Effect of Poly-L-lysine coating on titanium osseointegration: from characterization to in vivo studies. *J. Oral Implantol.* **2015**, *41*, 626−631.

https://dx.doi.org/10.1021/acsomega.0c00986
ACS Omega 2020, 5, 10562−10571